Universidad Zaragoza
1542

Bachelor's Thesis

"Generation of fluorescently labelled constructs for improvement of microscopy in 2D and 3D cultures"

Author:
África Temporal Plo

Director:
Vera Kozjak-Pavlovic
(University of Würzburg)

Year 2018/2019

I, Dr. Vera Kozjak-Pavlovic, from the University of Würzburg (Germany), authorize Ms. África Temporal Plo, biotechnology student from the University of Zaragoza (Spain), to present her finished Bachelor's Thesis: **Generation of fluorescently labelled constructs for improvement of microscopy in 2D and 3D cultures**. All the laboratory work was carried out at the laboratories of the Chair of Microbiology of the University of Würzburg (Germany).

Würzburg, 24 June 2019
Dr. Vera Kozjak-Pavlovic

List of abbreviations

ATCC	American Type Culture Collection
ATP	Adenosine triphosphate
bp	Base pairs
BSA	Bovine serum albumin
cDNA	Complementary DNA
CMV	Cytomegalovirus
CTP	Cytidine triphosphate
DMSO	Dimethyl sulfoxide
DNA	Deoxyribonucleic acid
EDTA	Ethylenediaminetetraacetic acid
FCS	Fetal calf serum
FFP	Fluorescent fusion protein
FPALM	Fluorescence Photoactivation Localization Microscopy
GFP	Green fluorescent protein
GTP	Guanosine triphosphate
IMM	Inner mitochondrial membrane
LB	Luria Bertani medium
MPP	Mitochondrial processing peptidase
NA	Numerical aperture
OD	Optical density
OMM	Outer mitochondrial membrane
OXPHOS	Oxidative phosphorylation
PALM	Photo-Activated Localization Microscopy
PAM	Translocase associated motor
PBS	Phosphate-buffered saline
PCR	Polymerase Chain Reaction
PFA	Paraformaldehyde
Prx	Peroxiredoxin
RNA	Ribonucleic acid
SIM	Structured Illumination Microscopy
STED	Stimulated Emission Depletion
STORM	Stochastic Optical Reconstruction Microscopy
TAE	Tris-Acetate-EDTA
TIM	Translocase of the inner membrane
Tm	Melting temperature
TOM	Translocase of the outer membrane
Tris	Tris-hydroxymethyl-aminomethane
TTP	Thymidine triphosphate
ZO1	Zonula occludens 1

Index

1. Abstract

Fluorescence microscopy is a very useful tool for biological research as it allows selective molecule labeling and life-cell imaging. In the last decades, the development of super resolution microscopy techniques has enabled us to gain a deeper insight into different biological processes. In any kind of fluorescence microscopy, correct molecule labeling is key to obtaining good quality images. In this project, two fusion proteins were designed to fluorescently label different cellular structures and show the potential of a super resolution microscopy technique known as SIM (Structured Illumination Microscopy).

First protein targeted was ZO1 (zonula occludens 1), which is located at epithelial cells tight junctions and has been reported to be important for *Neisseria gonorrhoeae* (*N. gonorroheae*) infection **[1]**. The goal was to fluorescently label ZO1 at its N-terminal domain, so it could be used in later studies about *N. gonorrhoeae* infection mechanism. The objective was to clone ZO1 at the C-terminal end of the fluorescent proteins mCherry and GFP, but ZO1 big size made amplification difficult and not enough amplified product was obtained to successfully transform *Escherichia coli* (*E.coli*) and clone it.

The other protein labelled was $F_1ß$, which forms part of the ATPase complex located at the inner mitochondrial membrane **[2]**. $F_1ß$ was fluorescently labelled at its C-terminal end with GFP and mCherry. Confocal fluorescent microscope images of the transfected HeLa cells demonstrated the correct colocalization of our protein with immunofluorescently labelled Tom20 and Peroxiredoxin 3 (Prx3). Mitochondria images taken with the SIM microscope showed the submitochondrial structure, distinguishing between outer mitochondrial membrane and inner membrane. These transfected cells can be used in later studies about submitochondrial protein localization.

Resumen

La microscopía de fluorescencia es una herramiento muy útil en la investigación biológica ya que permite el marcaje específico y el estudio de las células "*in vivo*". En las últimas décadas, el desarrollo de la microscopía de súper resolución ha permitido profundizar en el estudio de distintos procesos biológicos. En cualquier tipo de microscopía de fluorescencia, un correcto marcaje es clave para obtener imágenes de buena calidad. En este proyecto, se han diseñado dos proteínas de fusión para marcar fluorescentemente distintas estructuras celulares y mostrar el potencial de una técnica de microscopía de alta resolución conocida como SIM.

La primera proteína marcada fue ZO1, localizada en las uniones estrechas entre células epiteliales y que se ha visto que está implicada en el mecanismo de infección de *N. gonorrhoeae* **[1]**. El objetivo era marcar ZO1 fluorescentemente en su dominio N-terminal, para que pudiera ser utilizada en estudios posteriores sobre el mecanismo de infección de *N. gonorrhoeae*. Se intentó clonar en el extremo C-terminal de las proteínas fluorescentes mCherry y GFP, pero el gran tamaño de ZO1 dificultó la amplificación y no se obtuvo suficiente producto como para poder transformar *E.coli* y clonarla.

La otra proteína marcada fue $F_1ß$, la cual forma parte del complejo ATPasa localizado en la membrana interna mitocondrial **[2]**. $F_1ß$ fue marcada fluorescentemente en su extremo C-terminal con GFP y mCherry. Las imágenes de las células HeLa transfectadas tomadas con el microscopio confocal demuestran la correcta colocalización de nuestra proteína con Tom20 y Prx marcados inmunofluorescentemente. Las imágenes de las mitocondrias tomadas con el microscopio SIM muestran la estructura submitocondrial, distinguiendo entre las membranas externa e interna. Estas células transfectadas pueden ser usadas en estudios posteriores sobre la localización submitocondrial de proteínas.

2. Background

2.1. From conventional microscopy to super resolution techniques

Since its invention in 1595, light microscopy has played a major role in biological research. In 1665, Robert Hooke first described cells after visualizing them with a microscope. Then, two hundred years later, Schleiden and Schwann used light microscopes to describe individual cells as the fundamental unit of life, settling the bases of modern biology **[3]**. Many advances have ocurred in the microscopy field since then and new techniques have been developed, like phase contrast, fluorescence microscopy or electron microscopy among others.

A great advantage of light microscopy, which includes brightfield and fluorescence, is that it allows specific molecule labeling. In addition to molecule specific contrast, fluorescence microscopy also permits live cell imaging to study "*in vivo*" processes. Live-cell imaging is an important tool in the understanding of complex biological processes. However, because of their resolution limitations, light microscopy techniques are inadequate for visualizing the inner architecture of many subcellular structures **[4]**. The best resolution or, in other words, the smallest separation that two objects can have and still be discerned, which can be achieved with a light microscope is around 200 nm. This limitation is due to a physical phenomenon called the difraction limit and was first fully described and formalized by Ernst Abbe in 1873 **[5]**. Ernst Abbe stated that the smallest resolvable distance between two points using a conventional microscope may never be smaller than half the wavelength of the imaging light. Microscopes resolution can be calculated with the formula displayed at Fig.1.

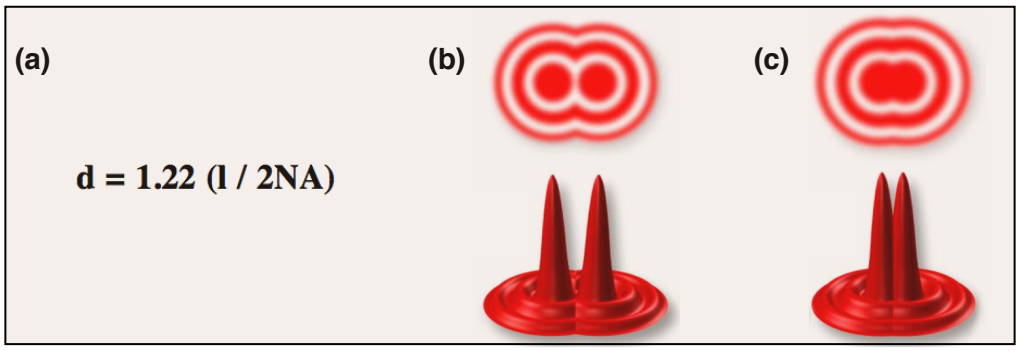

Fig.1. The diffraction limit. (a) Rayleigh resolution equation. d=space between two adjacent particles (still allowing the particles to be perceived as separate). l=wavelength of illumination. NA=numerical aperture of the objective. **(b)** Two spots at the limit of resolution. **(c)** Two spots so close together that their central spots overlap.
From *Optical Microscopy*, Michael W. Davidson and Mortimer Abramowitz **[6]**

In order to improve the resolution, other techniques such as electron microscopy (where photons are replaced with electrons) have been developed. Electrons have a much lower wavelength than light, for this reason, the maximun resolution that can be achieved with an electron microscope is 0,1 nm, two orders of magnitude smaller than the resolution achieved with conventional light microscopes. However, electron microscopy does not allow "*in vivo*" imaging and is generally less capable than light microscopy of determining the distribution of individual proteins. Immunolabeling with gold conjugated antibodies is usually the method of choice to determine protein localization using electron microscopy, but it remains challenging and only a very small fraction of the target protein is detected. **[7]**

In the last decades, new approaches to try and break the resolution limit have been made, resulting in the development of a new generation of microscopes known as super resolution microscopes. The use of these new methods has been extended to different biological fields and its potential has been tested **[8][9]**. In this project super resolution microscopy techniques were applied to two different biological areas: cell biology (potential for visualizing submitochondrial protein distributions) and microbiology (fluorescent labeling of proteins involved in *N. gonorrheae* infection mechanism).

2.1.1. Super resolution microscopy

As stated before, fluorescence microscopy resolution (wide field and laser scanning) cannot surpass the so called diffraction limit. The size of the fluorescence spots is determined by the wavelength of the fluorescence and affects the spatial resolution. This means that if two fluorescent spots are separated by a distance lower than the diffraction limit they will appear as a single object, making them unresolvable from each other **[10]**. Super resolution techniques use the physical properties of fluorescent probes to distinguish emissions from two nearby molecules within a diffraction limited region. These methods can be divided into two primary classes: ensemble imaging approaches and single-molecule imaging. **[11]**

Ensemble imaging approaches use patterned illumination to spatially modulate the fluorescence behaviour within a diffraction-limited region (Fig.2). Not all of the molecules emit simultaneously, thereby achieving subdiffraction limit resolution. An example of this type of microscopes are STED (stimulated emission depletion) and SIM (structured illumination microscopy). The main difference between STED and SIM is that STED uses negative patterning while SIM uses positive patterning.

On the other hand, single-molecule imaging is based on the activation of individual molecules within the diffraction-limited region at different times. Measuring the position of individual fluorophores, images with subdifraction limit resolution can be reconstructed. STORM (Stochastic Optical Reconstruction Microscopy), PALM (Photo-Activated Localization Microscopy) and FPALM (fluorescence photoactivation localization microscopy) are super resolution techniques that utilize this approach. STORM and (F)PALM requirements put several constraints on the fluorescent probes.

In this proyect we have used a SIM (Structured Illumination Microscopy) microscope. SIM increases spatial wide field resolution by a factor of two, reaching a resolution of aproximately 100 nm in the lateral dimensions. SIM permits labeling using conventional fluorophores and imaging of up to three colours simultaneously. **[11]**

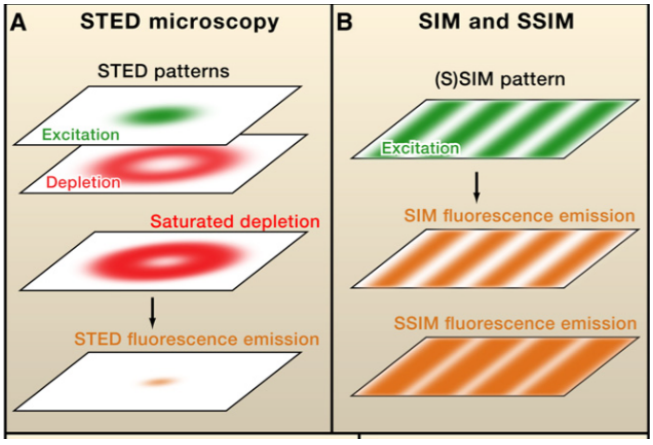

Fig.2. Super-Resolution Fluorescence Microscopy by Patterned Illumination. A. STED microscopy. Excitation light beam (green), additional depletion light beam (red). The depletion effect reduces the size of the fluorescent spot (orange), improving the image resolution. **B**. SIM and saturated SIM (SSIM) microscopy. Excitation patterned illumination (green). Fluorescence emission pattern (orange). From *Breaking the diffraction barrier: Super-resolution imaging of cells,* Bo Huang, Hazen Babcock, and Xiaowei Zhuang **[11]**.

There are two major fluorescence labeling methods: immunolabeling (or immunofluorescence) and fusion proteins. Immunolabeling consists in targeting proteins with fluorophore-labelled antibodies. The fluorophore can be directly conjugated to the primary antibody or instead of that, to the secondary antibody, which will recognize the primary antibody attached to the protein of interest. The accuracy of protein recognition depends on the specificity of the primary antibody. A disadvantage of immunolabeling is that usually it requires cell fixation and permeabilization **[12]**. In contrast, when labeling with a fusion fluorescence protein, the target protein and the fluorophore are covalently fused and the chimeric protein is endogenously expressed by the cell, allowing "*in vivo*" imaging. **[13]**

2.2. Super resolution microscopy as a tool to study *N. gonorrhoeae* infection

Gonorrhea is an infectious disease primary involving the genitourinary tract. The disease is caused by the small gram negative diplococcus *N. gonorrhoeae*, whose only natural hosts are humans. Transmission is most commonly caused by some form of sexual contact, and infection usually occurs in the more sexually active age groups. Concerning the infection mechanism, it has been suggested that in females the infection initiates at the endocervix, and may lead to pelvic inflammatory disease if it remains untreated **[14]**. Endocervix is composed of a monolayer of polarized columnar epithelial cells sealed by apical junctions complexes, which comprise tight junctions and adherens junctions. Tight junctions are the most apical structure of the complex and adherens junctions are positioned immediately below them. Tight junctions and adherens junctions detailed structure has been expertly reviewed elsewhere. **[15]**

Apical junctions form a tight seal between adjacent cells, providing a barrier to the diffusion of solutes through the paracellular pathway (gate function), and keeping proteins and lipids in the apical and lateral membrane from moving to the other side (fence function). This barrier also confers protection from pathogenic microorganisms, preventing them from penetrating into deeper tissues. However, some pathogens, like *N. gonorrhoeae*, have developed different ways to disrupt this barrier, enter through it and colonize the subepithelium space.

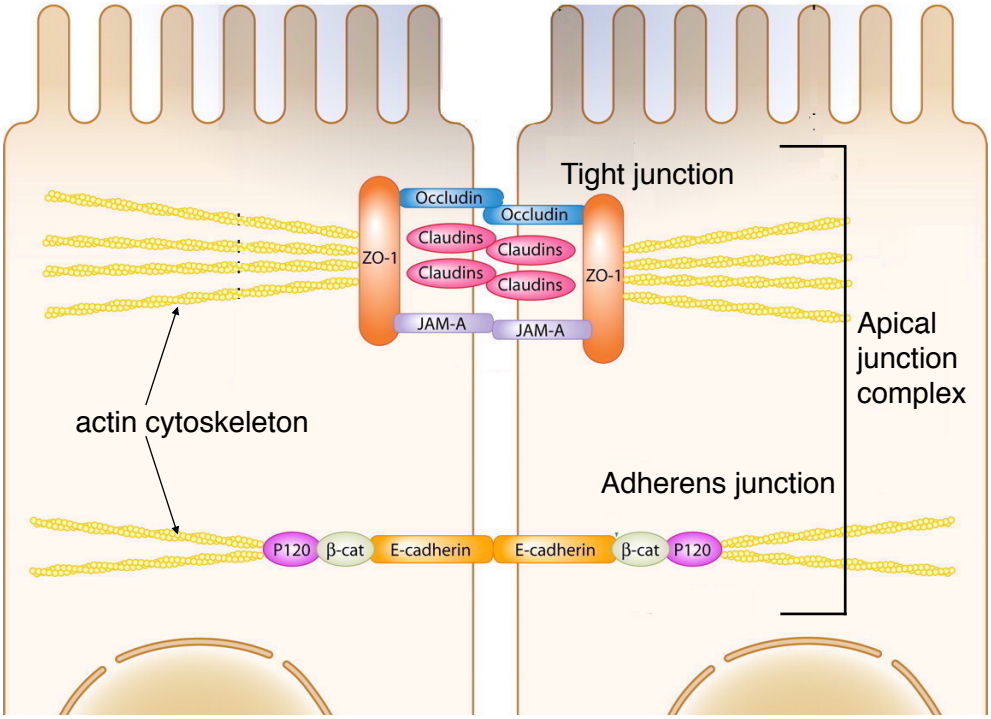

Fig.3. Apical junctional complexe structure. Adapted from *Helicobacter pylori and Gastric Cancer,* Wroblewski LE, Peek RM, Wilson KT **[16]**

N. gonorrhoeae can break the endocervix epithelial barrier by the dissasembly of apical junctions and the induction of columnar epithelial cells exfoliation. The disassembly is due to the dissociation of ZO1 and ß-catenin from the junctional complex induced by *N. gonorrhoeae* interaction. In *N. gonorrhoeae* infected cells, ZO1 and E-cadherin are redistributed from the apical junction to the cytoplasm and intracellular vesicles respectively, facilitating *N. gonorrhoeae* transmigration **[14]**. ZO1 is involved in the formation of tight junctions and together with ZO2 and ZO3, belongs to the superfamily of MAGUK proteins. ZO1 links tight junction transmembrane proteins to the actin cytoskeleton. The N-terminal amino acids (633–896) of ZO1 are required for its association with tight junctions **[17]**. However, the C-terminal region (amino acids 1151-1372) is an actin-binding region that interacts directly with F-actin and has an important role in the localization of ZO1 at junctions, promoting the stabilization of ZO1 within cell–cell contacts. **[18]**

The exact mechanism of how *N. gonorrhoeae* breaks the epithelial barrier and transmigrates across the epithelial monolayer remains unknown. To adress this question, development of 3D tissues mimicking the endocervix in combination with fluorescent labeling of ZO1 and super resolution microscopy could be used to study the "*in vivo*" dynamics of tight junctions after *N. gonorrhoeae* infection.

2.3. Super resolution microscopy of mitochondria

Mitochondria are essential organelles for eukaryotic cells. They synthesize the majority of ATP needed in cells and are involved in other important metabolic processes, including biosynthesis of amino acids, lipids, heme, and Fe-S clusters. They also play crucial functions in cellular signaling pathways, quality control, and programmed cell death. Mitochondrial structure consists of an outer (OMM) and inner membrane (IMM) that separate two aqueous compartments, the intermembrane space and the matrix. The inner membrane contains invaginations referred to as cristae, which is where oxidative phosphorylation occurs.

Mitochondria's small size (width 250nm aproximately) makes the analysis of submitochondrial protein distribution often impossible using conventional fluorescence microscopy. For this reason, mitochondrial biology has been at the focus of super resolution microscopy since its beginnings **[19]**. In order to visualize the submitochondrial structure it is necessary to decide which proteins are going to be labelled and the labeling method. In many studies, the chosen protein has been Tom20, which is a subunit of the translocase of the mitochondrial outer membrane (TOM) complex **[20][21][22]**. Other studies have succesfully imaged cristae, although they remain a more challenging target because of their small size and complex structure. For example, in *Mitochondrial Cristae Revealed with Focused Light* (Roman Schmidt, et al.), the F_1F_0ATPase complex was labelled with a fluorophore-conjugated antibody, and STED images of mitochondria showing cristae were taken (Fig. 4) **[23]**. Other labeling option would be the construction of a fusion protein. In this case, it is important to know whether the gene is encoded by the nucleus or by the mitochondrial genome.

Although mitochondria have kept their own genome and protein synthesis machinery, most of endosymbiont genes have been transferred to the nucleus. Human mitochondrial genome codes for 13 core subunits of the respiratory chain. Mitochondrial proteins encoded by nuclear genes are synthesized in the cytosol and contain targeting signals that direct them to mitochondria and into the right mitochondrial compartment. Five major protein import pathways have been described, each of them characterized by the targeting signal. Most mitochondrial proteins are synthesized in the cytosol with a cleavable N-terminal presequence. Proteins carrying the N-terminal presequence are imported by TOM (translocase of the outer membrane) and TIM23 (translocase of the inner membrane). After protein translocation into the matrix mediated by PAM (translocase associated motor), the N-terminal presequence is cleaved off by MPP (mitochondrial processing peptidase). **[24]**

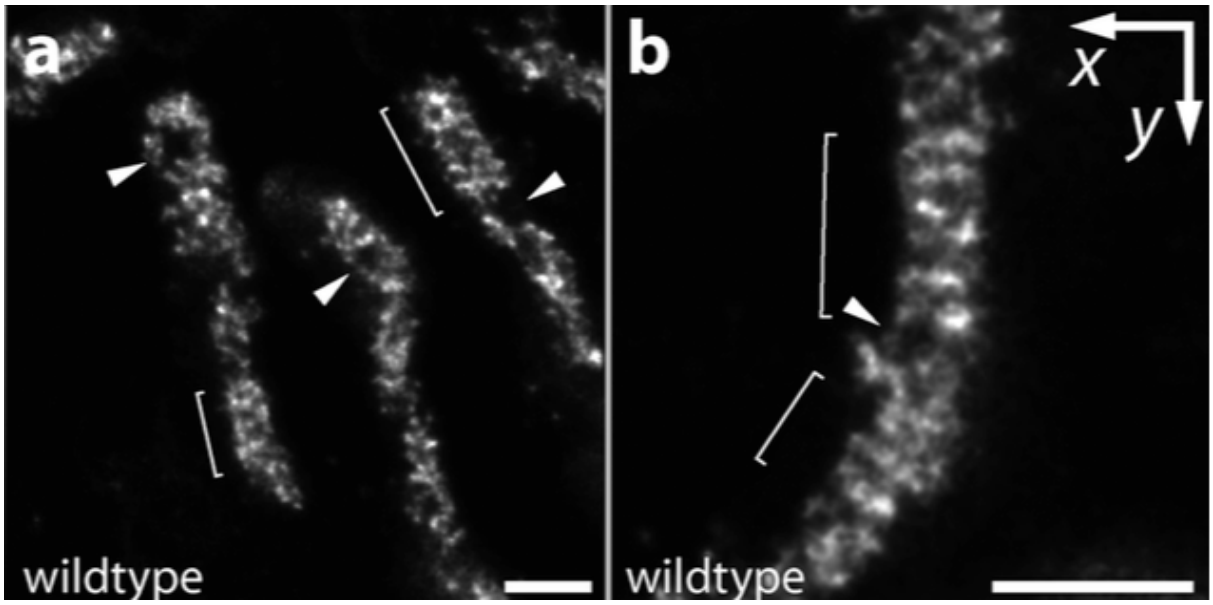

Fig.4. IsoSTED nanoscopy images recorded of mitochondria. (a) Overview and (b) close-up of mitochondria recorded at their equatorial planes in the interior of an intact cell. The IMM was labeled with antibodies directed against the F_1F_0ATPase. Cristae perpendiularly oriented to the longitudinal mitochondrial axis are indicated with brackets. Arrowheads point to inner-mitochondrial regions in which there are no cristae. Scale bars: 500 nm. From *Mitochondrial Cristae Revealed with Focused Light*, Schmidt R, et al. **[23]**

3. Objectives

The main goal was to obtain two fluorescent fusion proteins which could be used in later biological studies that required the utilization of super-resolution microscopy. The proteins of interest were ZO1 and $F_1ß$:

ZO1

- Explore the methodology to construct a fusion protein to fluorescently label ZO1, so it permits the study of *N. gonorrhoeae* infection mechanism.

$F_1ß$

- Construction of a fusion protein to fluorescently label $F_1ß$.
- Co-localization of fluorescent $F_1ß$ with Tom20 and Prx labelled with antibodies.
- Comparison of mitochondria pictures obtained with confocal microscopy and super resolution microscopy.
- Visualization of the inner structure of mitochondria.
- Obtention of cells transiently expressing $F_1ß$ that can be used in later studies about submitochondrial protein distribution and dynamics.

4. Materials and methods

4.1. Cell culture

Bacterial strains and cell lines utilized in this work, as well as their characteristics and source, are collected in the supplementary material (Table 1S).

DH5α competent *E. coli* were distributed in 200 µl LB (Luria Bertani) liquid medium aliquots and stored in the freezer at -80 ºC until needed. After transformation, bacteria were seeded in agar plates containing LB medium and ampicillin.

LB liquid medium was prepared mixing 10 g tryptone with 5 g yeast extract and 5 g NaCl and then adding distilled H_2O until a final volume of 1 L was reached. Then it was autoclaved and stored at 4 ºC. For the solid medium, 20 g agar were added to the mixture.

HeLa 2000 (used for total RNA purification) and HeLa 229 (used for transfection) cells were grown in RPMI medium containing 10% fetal calf serum (FCS).

Table 2S of the supplementary material shows all the comercial media used as well as the company that provided them.

4.2. cDNA isolation

4.2.1. Total RNA purification

To purify total RNA from HeLa 2000 cells, miRNeasy Micro Kit (from QIAGEN) was used. The protocol provided by QIAGEN was followed without variations.

4.2.2 Conversion of RNA to cDNA

The reagents and their concentration are listed in Table 1. All the reagents were mixed and then incubated 60 min at 42 ºC. Then, they were incubated for another 5 min at 70 ºC. The cDNA concentration was measured with a nanodrop spectrophotometer and the solution was distributed in 10 aliquots of 2 µl each ([cDNA] = 4317,6 ng/µl) and stored in the freezer at -80 ºC until needed. To check cDNA quality, a PCR with primers to amplify GADPH was performed. The results were positive, so the cDNA could be used for cloning.

Reagent	**Volume**
RNA (5210 µg/µl)	1 µl
oligo $(dt)_{18}$ primer	1 µl
DEPC-treated water	10 µl
5x Reaction buffer	4 µl
RiboLock™ RNase Inhibitor	1 µl
10mM dNTP Mix	2 µl
Revert Aid™ M-MuLV Reverse Transcriptase	1 µl

Table 1. DNA synthesis reagents

4.2.3. Nanodrop spectrophotometer

Nucleotides (RNA, DNA) quantity and purity were measured with a nanodrop spectrophotometer from Peqlab Biotechnology, which, together with the rest of the equipment used, is listed in Table 5S (supplementary material).

4.3. Polymerase Chain Reactions (PCRs)

4.3.1 Expand long Template PCR System

This system from Sigma-Aldrich is useful to amplify long fragments. It was used to amplify ZO1 (5 kb) from total HeLa cDNA. The protocol provided by Sigma-Aldrich was followed without variations and the programme used was the following: initial denaturalization (2 min 94 ºC). 30 amplification cycles (denaturing 15 s 94 ºC, ealing 30 s 54 ºC, extension 4 min 68 ºC). Final extension: 7 min 68 ºC. After that, the probes were maintained at 4 ºC. The primers are listed in Table 3S (supplementary material).

4.3.2. Phusion PCR

Thermo Scientific Phusion High-Fidelity DNA Polymerase kit was used to amplify ZO1 (5 kb) from total HeLa cDNA. Phusion DNA polymerase has a determined error rate of 4,4 x 10^{-7} and is capable of amplifying long amplicons. It was proceeded according to the manufacturer's instructions. This method was also utilized to amplify the insert with AQUA-cloning primers. The primers were the same used in the previous method (Table 3S).

The programme used was the following: initial denaturalization (1 min 98 ºC). 30 amplification cycles (denaturing 10 s 98 ºC, annealing 10 s 54 ºC, extension 3 min 72 ºC). Final extension: 5 min 72 ºC. After that, the probes were maintained at 4 ºC.

4.3.3 Taq polymerase PCR

Taq polymerase PCR was utilized for colony screening, for DH5α competent cells checking and for total cDNA integrity checking.

The reagents for one probe were: forward primer (0,5 µl), reverse primere (0,5 µl), dNTPs (0,5 µl), 10x amplification buffer (5 µl), *Taq* polymerase (0,25 µl) and H_2O (38,35 µl).

The programme used was the following: initial denaturalization (3 min 94 ºC). 30 amplification cycles (denaturing 30 s 94 ºC, annealing 30 s 50 ºC, extension 3 min 72 ºC). Final extension: 10 min 72 ºC. After that, the probes were maintained at 4 ºC.

4.3.4. iProof polymerase PCR

iProof High Fidelity DNA polymerase from Bio-Rad was used for $F_1ß$ amplification from total HeLa cDNA. iProof error rate is very low, 50 times lower than that of *Thermus aquaticus* polymerase and 10 times lower than that of *Pyrococcus furiosus* polymerase. The protocol provided by Bio-Rad was followed without variations. The primers are listed in table 4S (supplementary material).

The programme used for $F_1ß$ amplification was the following: initial denaturation (30 s 98 ºC). 30 amplification cycles (denaturing 10 s 98 ºC, annealing 10 s 55 ºC, extension 1 min 72 ºC). Final extension: 5 min 72 ºC. After that, the probes were maintained at 4 ºC.

4.4. Cloning techniques

4.4.1. Plasmids

Plasmids utilized were derived from the vector pcDNA3, which is a mamalian expression vector with a CMV (cytomegalovirus) promoter and ampicillin resistance. Plasmids are listed and characterized in the following table:

Plasmid	Characteristics	Source
pcDNA3-mCherryM	pcDNA 3 with a N-terminal mCherry fluorescent tag	Elke Maier
pcDNA3-GFPM	pcDNA 3 with a N-terminal GFP fluorescent tag	Elke Maier

pcDNA3-mCherryS	pcDNA 3 with a C-terminal mCherry fluorescent tag	Elke Maier
pcDNA3-GFPS	pcDNA 3 with a C-terminal mGFP fluorescent tag	Elke Maier

Table 2. Plasmids

4.4.2. DISEC-TRISEC

Di- and trinucleotide-sticky-end cloning of PCR-amplified DNA (DISEC-TRISEC) facilitates directional cloning of PCR products. This method is based on the generation of complementary sticky ends at the linearized vector and the PCR amplified DNA. The vector is subjected to a "fill in" reaction and the insert to a "trim" reaction. The method is described in detail in Fig. 5. The example displayed represents the process using the restriction enzymes *Eco*RI and *Xho*I because they were utilized for ZO1 cloning.

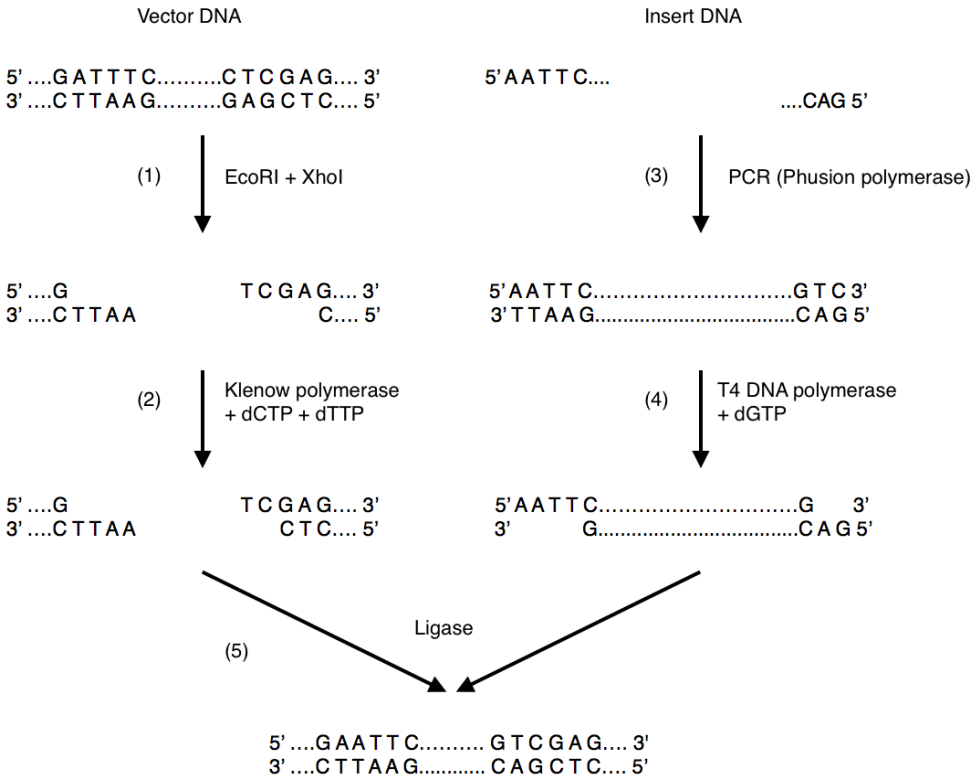

Fig. 5. DISEC-TRISEC. Schematic representation of the method. This example shows the steps followed to clone ZO1.

Klenow polymerase has polymerase activity 5'-3' and exonuclease activity 3'-5'. T4 DNA polymerase has polymerase activity 5'-3' and exonuclease activity 3'-5'. Before ligation, it is necessary to purify the vector and the insert.

The primers used for the amplification of ZO1 and $F_1ß$ are listed in Table 3S and Table 4S (supplementary material).

For the vector fill-in reaction 3-5 µg of the plasmid are needed, and for the insert trim reaction 2-3 µg DNA. The total volume for each of the reactions was 50 µl.

ZO1: Construction of chimeric ZO1-GFPM and ZO1-mCherryM

ZO1 was cloned into mCherryM-pcDNA 3 vector and GFPM-pcDNA3 vector. To cut the vector restriction enzymes *Eco*RI and *Xho*I were used.

Vector fill-in reaction mix: 2,5 µl dCTP (20 mM) and 2,5 µl dTTP (20 mM), 1,25 µl Klenow polymerase (100 U/µl), 5 µl 10x Klenow buffer, 30 µl mCherryM-pcDNA3 (160 ng/µl), 8,75 µl H_20.

For GFPM-pcDNA3 28 µl of the vector (110 ng/µl) were added, and H_20 was adjusted to have a final volume of 50 µl.

Insert trim reaction mix: 4 µl dGTP (20mM), 8 µl T4 polymerase buffer, 4 µl 10x BSA, 0,5 µl T4 polymerase and 30 µl ZO1 (91,9 ng/µl), 3,5 µl H_20.

F_1ß: Construction of chimeric F_1ß-GFPS and F_1ß-mCherryS

F_1ß was cloned into mCherryS-pcDNA 3 vector and GFPS-pcDNA3 vector. The restriction enzymes used were *BamI* and *HindIII*-HF. For the vector fill-in reaction dATP and dGTP were mixed, and for the insert trim reaction dCTP was used.

Vector fill-in reaction mix: 2,5 µl dATP (20 mM) and 2,5 µl dGTP (20 mM), 1,25 µl Klenow polymerase (100 U/µl), 5 µl 10x Klenow buffer, 35,5 µl mCherryS-pcDNA3 (84,3 ng/µl), 3,25 µl H_20.

For GFPS-pcDNA3 27,5 µl of the vector (109,5 ng/µl) were added, and H_20 was adjusted to have a final volume of 50 µl.

Insert trim reaction mix: 4 µl dCTP (20 mM), 8 µl T4 polymerase buffer, 4 µl 10x BSA, 0,5 µl T4 polymerase and 30 µl F_1ß (82,1 ng/µl), 3,5 µl H_20.

4.4.3. DNA purification

To purify the insert and the vector after PCR and DISEC-TRISEC reaction, the kit PureLink™ PCR Purification Kit (Thermo Fisher Scientific®) was used. It was proceeded according to the manufacturer's instructions.

4.4.4. DNA electrophoresis

The electrophoresis gel used had 1% agarose. Agarose was dissolved in 1X TAE (Tris-Acetate-EDTA) buffer (1,5 g agarose / 150 ml 1X TAE), and after it cooled down a little 10 µl of SYBR Green were added to stain the DNA.

The loading buffer was 6x Loading Dye Solution (Fermentas) and the molecular weight size marker was 1 kb DNA ladder from Fermentas.

The electrophoresis were run under the following conditions: 160 V, 400 mA, 35 min.

4.4.5. DNA ligation

After purifying DISEC-TRISEC vector and insert, they were assembled with a ligation reaction. The ratio was 1:4 (vector:insert).

ZO1:

ZO1-GFPM: 2,8 µl ZO1 [118,3 ng/µl] + 2,2 µl GFPM pcDNA3 [44,7 ng/µl] + 2 µl 10x T4-Ligasebuffer + 1 µl T4 ligase + 12 µl H_2O

ZO1-mCherryM: 3,5 µl ZO1 [118,3 ng/µl] + 1,5 µl mCherryM [78,4 ng/µl] + 2 µl 10x T4-Ligasebuffer + 1 µl T4 ligase + 12 µl H_2O

F_1ß:

F_1ß-GFPS: 4,8 µl F_1ß [82,1 ng/µl] + 2,2 µl GFPS pcDNA3 [102,4 ng/µl] + 1,5 µl 10x T4-Ligasebuffer +1 µl T4 ligase + 5,5 µl H_2O

F_1ß-mCherryS: 4,6 µl F_1ß [82,1 ng/µl] + 2,4 µl mCherryS pcDNA3 [84,3 ng/µl] + 1,5 µl 10x T4-Ligasebuffer +1 µl T4 ligase + 5,5 µl H_2O

4.4.6. AQUA Cloning

AQUA (Advanced Quick Assembly) cloning is an enzyme-free cloning method. It is based on the principle of *in vivo* cloning in *E. coli.* **[25]**

DNA inserts need to share from 16 to 32 base pairs (bp) of homologous sequence with each adjacent vector DNA fragment. *E. coli* is transformed with the prepared insert and the vector and then it assembles both parts.

Aqua mixture: the insert-vector ratio is 3:1 in a total volume of 10 µl. After mixing the components it is necessary to incubate 1 hour at room temperature. 5 µl of the mixture are necessary to transform 25 µl of competent *E. coli* Top10. As explained in the Results section, this method was not completly performed. Primers utilized for this method are collected in Table 3S (supplementary material).

4.5. Cell transformation

4.5.1. Preparation of competent cells

Competent *E. coli* DH5α cells were obtained with the $CaCl_2$ technique. An overnight *E.coli* DH5α culture was diluted 1:100 to start a subculture, when the OD (optical density) of the subculture reached aproximately 0,4, it was washed with a $CaCl_2$ solution. After the washing, the supernatant was discarded and the pellet was resuspended in a 0.1 M $CaCl_2$ solution with 5% DMSO. This solution was distributed in 100 µl aliquots and freezed at -80 ºC until bacteria were needed for transformation procedures.

4.5.2. Transformation of DH5α cells

100 µl of an aliquot of competent *E. coli* DH5α cells were mixed with 15 µl of the ligation product. Bacteria were transformed with heat shock (30 min on ice, 90 s at 42 ºC, 2 min on ice). After that, 1 ml LB medium was added and cells were grown on a shaking incubator at 37 ºC for 45 min. After that, bacteria were seeded in LB-medium agar plates that contained ampicillin. Transformed cells were incubated overnight at 37 ºC.

4.5.3. Colony screening

The overnight culture of transformed *E. coli* colonies was analyzed, with PCR and electrophoresis, to check if there was any colony that had incorporated the plasmid with the insert. For the PCR, the DNA polymerase used was *Taq* (as explained in the section 4.3.3.).

4.5.4. Plasmid extraction

Plasmids were extracted from the positive colonies detected at the colony screening. The extraction was performed utilizing a Miniprep kit from Thermo Fisher Scientific® according to the manufacturer's instructions.

4.5.5. Sequencing

In order to check that the plasmids contained the right insert before transfecting the HeLa cells, they were sent to Microsynth Seqlab for sequencing. Sequencing primers are listed in Table 4S (supplementary material).

4.5.6. Transfection of HeLa229 cells with VIROMER

VIROMER is a transfectant agent from Lipocalyx®.

Cells were seeded on wells and grown over night.The next day, the transfection mixture was prepared and 100 µl of it were added per well. The transfection mixture was the result of combining the content of eppis 1 and 2:

> Eppi 1: 90 µl buffer + 1 µg DNA (2,3 µl F_1ß-mCherryS [436,3 ng/µl], or 2,7 µl F_1ß-GFPS [370,8 ng/µl]).

Eppi 2: 0,3 µl VIROMER + 9,7 µl VIROMER Buffer. After mixing both vortex 10 s.
Eppi 1 content was added to Eppi 2. After 15 min the transfection mixture was added to the wells.
The immunofluorescence staining was performed two days after the transfection to allow the transfected cells to grow and start expressing the fusion protein.

4.6. Fluorescence microscopy

4.6.1. Immunofluorescence—Staining

HeLa 229 cells were immunostained after being previously transfected with F_1ß-mCherryS or with F_1ß-GFPS.
The primary antibodies used were mouse Tom20 and rabbit Prx3. Secondary antibodies depended on the fluorescent tag of the fusion protein: for the cells transformed with F_1ß-mCherryS (red), secondary antibodies used were mouse Cy2 (green) and rabbit Cy5 (blue); for the cells transformed with F_1ß-GFPS (green), secondary antibodies used were mouse Cy3 (red) and rabbit Cy5 (blue).
Cells were fixed with 3% PFA (30 min incubation at 37ºC). After fixation, cells were washed with PBS and then the blocking buffer was added (10 % goat serum 0.2 % Triton X-100 in 1X PBS). After 30 min of incubation with the blocking buffer, cells were washed again with PBS. Then, they were incubated with the primary antibody dilution for 1 h and washed with PBS. Cells were then blocked for another 10 min in the blocking buffer at room temperature and washed with PBS. After that, the cells were incubated with the secondary antibody dilution and washed again with PBS.
Antibodies dilution solutions were the following:

- Tom20 dilution solution: 3% goat serum, 0,01% Tom20 in PBS (1:100 dilution, 1,2 µl in a total volume of 120µl). 30 µl were added per well.
- Prx3 dilution solution: 3% goat serum, 0,003% Prx 3 in PBS (1:300 dilution, 0,4 µl in a total volume of 120µl). 30 µl were added per well.
- Cy2, Cy3, Cy5: 3% goat serum, 0,003% Cy in PBS (1:300 dilution, 0,4 µl in a total volume of 120µl). 30 µl were added per well.

4.6.2. *Confocal Microscopy*

Confocal microscopy was used to visualize cells after they were transformed and immunostained. The microscope utilized was Leica TCS SPE confocal microscope. Its maximun resolution is 200 nm and it enables the simultaneous imaging of up to four different wavelengths.

4.6.3. Structured illumination microscopy (SIM): Zeiss Elyra

Cells were also visualized with high resolution microscopy. The microscope utilized was Zeiss Elyra. As discussed in the introduction, there are different techniques of high resolution microscopy. Zeiss Elyra has integrated two of these methods: SR-SIM (structured illumination microscopy) and PALM (photoactivated localization microscopy). Despite their similarities, each of them belongs to a different super resolution microscopy class. The highest resolution that can be achieved with Elyra is 20 nm, using PALM.
Images were taken with the SR-SIM method.

4.6.4. Image processing: Fiji

Both confocal and SIM microscope images were processed with the image processing package Fiji (Image J). **[26]**

5. Results

5.1. Protein ZO1 (Zonula occludens 1)

In order to study *N. gonorrhoeae* infection mechanism in a 3D model of the human endocervix, ZO1 protein was chosen to be fluorescently labelled with mCherry or GFP. The goal was to obtain a construct that could be used in later studies to visualize how *N. gonorrhoeae* infection affects tight junctions.

5.1.1 Construction of the fusion protein

ZO1 is 5210 pb long. When a fragment's size exceeds 5 kb, basic PCR efficiency decreases significantly, which can be due to the accumulation of truncated products. For this reason, different comercial systems and conditions for long fragment PCR amplification were tested. The DNA template used was total cDNA extracted from HeLa cells.

5.1.1.1. Expand Long Template PCR System

This system from Sigma-Aldrich® contains two thermostable enzymes: *Taq* Polymerase and a polymerase with 3'—>5' exonuclease activity (proofreading activity). The proofreading polymerase is added to remove the nucleotide misincorporations that may interfere with strand synthesis, which allows *Thermus aquaticus* (*Taq*) polymerase to complete DNA synthesis.**[27]**

There was no 5 kb band in the electrophoresis results, so there had been no ZO1 amplification (results not shown). Two different polymerase comercial buffers (1 and 2) were tried, but the results were the same.

5.1.1.2. Phusion polymerase

Phusion polymerase was the second DNA polymerase for long fragment amplification tested.

Phusion DNA polymerase from New England BioLabs® was generated fusing a DNA-binding domain with a *Pyrococcus*-like polymerase. It has a very low error rate, about 50-fold lower than that of *Taq* DNA polymerase, as stated in the product information provided by Thermo Scientific. This time there was no amplification either (not shown).

5.1.1.3. Phusion polymerase + DMSO

DMSO is a solvent commonly used in standard PCR. It improves the reaction yield and specificity. It has been described how it can also facilitate long PCRs. **[27]**

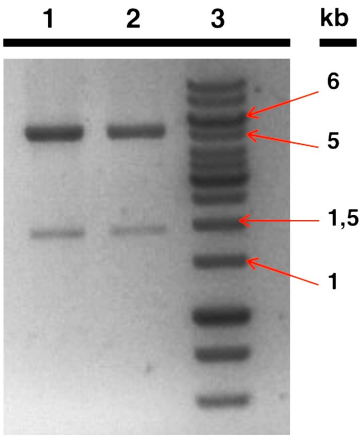

Fig.6. Phusion polymerase + 2 µl DMSO PCR. Lane 1: ZO1 amplification. Lane 2: ZO1 amplification. Lane 3: molecular-weight size marker.

Two different bands can be seen in lanes 1 and 2 in Fig. 6. The upper band is between 5 and 6 kb, which corresponds with ZO1 size: 5210 pb.
The other band's size is 1,5 kb and may be a nonspecific amplification product.
This was the only method that allowed ZO1 amplification using the DISEC-TRISEC primers.

5.1.2. Transformation

5.1.2.1. DISEC-TRISEC

DISEC-TRISEC was the first cloning method attempted. This method is explained in detail in *Materials and Methods*. The basic steps of DISEC-TRISEC are designing the right primers and choosing the correct insert trim reaction and vector fill in reaction. If done so, an insert and vector with complementary sticky ends are obtained without using any restriction enzyme to cut the insert. In order to cut the vector, two different enzymes were used: *Eco*RI and *Xho*I.
This technique is particularly useful if the insert contains the restriction site of the enzyme one wants to cut the vector with, or when one doesn´t know the sequence of the fragment one wants to amplify.
As shown in the Fig. 6, ZO1 was amplified using the DISEC-TRISEC primers. After that, *E. coli* DH5α competent cells were transformed with the amplified insert and the vector.
No colonies transformed with the plasmid and the insert were obtained.

5.1.2.2. AQUA Cloning

Since *E.coli* DH5α weren't transformed using DISEC-TRISEC, another cloning method was tested: AQUA-cloning.
AQUA Cloning is a ligase-independent cloning strategy. Instead of doing the ligation *in vitro* and after that the bacterial transformation, bacteria are transformed with the insert and the vector and then they assemble them *in vivo*. For this reason, the ends of the amplified insert have to be homologous with the ends of the cut vector. As explained in *Materials and Methods*, from 16 of 32 homologous base pairs (bp) are needed. This makes necessary the utilization of long primers, in our case 38 (forward) and 37 (reverse) nucleotides, which can lower PCR efficiency. Since the amplification wasn't successful, transformation using this method couldn't be attempted.

5.2. Protein $F_1ß$

Our goal was to create a construct that allowed the visualization of the individual distribution of proteins in the mitochondria. For that purpose, a fusion protein was created through the joining of $F_1ß$ and a fluorescent protein (GFP or mCherry). In order to study the correct localization or our fusion protein, co-localization studies labeling Tom20 (mitochondrial outer membrane protein) and Prx (mitochondrial matrix membrane) with antibodies were carried out. Two different fusion proteins were created (F1ß-mCherry and F1ß-GFP) to compare them and check which one gave the strongest signal.

Pictures were taken with a confocal microscope and a super resolution microscope. As discussed in the Introduction, only the super resolution microscope allows the visualization of submitochondrial protein distribution. Fig. 10 (Leica TCS SPE confocal microscope) and Fig. 11 (SIM Zeiss Elyra) show the resolution difference between these two microscopy techniques.

5.2.1. Construction

The outcome of the experiment depended on the correct DNA sequence, so to minimize the incorporation of mismatched nucleotides a high fidelity polymerase was utilized in the amplification: iProof polymerase.

The amplification primers were designed according to DISEC-TRISEC cloning method, which allows directional cloning. This method as well as the primers are described in detail at *Materials and Methods* section. $F_1ß$ was amplified from HeLa total cDNA.

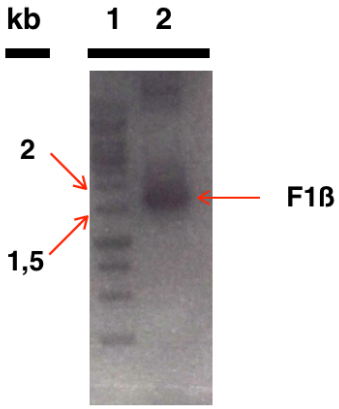

Fig. 7. $F_1ß$ PCR. Lane 1: molecular-weight size marker. Lane 2: $F_1ß$ amplification.

Fig. 7 shows a band between 1,5 and 2 kb, which corresponds to $F_1ß$ size: 1.8 kb **[28]**. There are also other bands resulting from nonspecific amplification.

5.2.2. Transformation

DH5α competent *E. coli* cells were transformed with two different constructs, both of them obtained with DISEC-TRISEC method (*Materials and Methods*). The constructs were: $F_1ß$-mCherryS-pcDNA3 and $F_1ß$-GFPS-pcDNA3.

Transformed colonies were selected with colony screening. Colony screening results are displayed in Fig. 8 and Fig. 9.

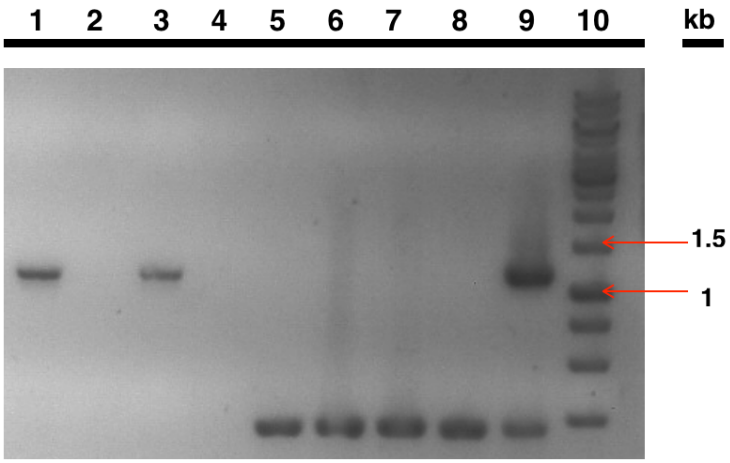

Fig. 8. F1ß-mCherryS-pcDNA3 and F1ß-GFPS-pcDNA3 *E. coli* colony screening.
Lanes 1-4: mCherryS. Lane 1: clone 2. Lane2: clone 3. Lane 3: clone 4. Lane 4: clone 5. Lanes 5-9: GFPS. Lane 5: clone 26. Lane 6: clone 27. Lane 7: clone 28. Lane 8: clone 29. Lane 9: clone 30. Lane 10: molecular-weight size marker.

Fig. 8 shows three positive results: clones 2 and 4 (F1ß-mCherryS); and clone 30 (F1ß-GFPS). To confirm that the constucts had the correct DNA sequence, clone 2 and clone 30 plasmids were extracted and sent for sequencing. Plasmid extracted from clone 2 (F1ß-mCherryS) had F_1ß sequence conserved. Plasmid extracted from clone 30 (F_1ß-GFPS) did not have F_1ß sequence conserved.

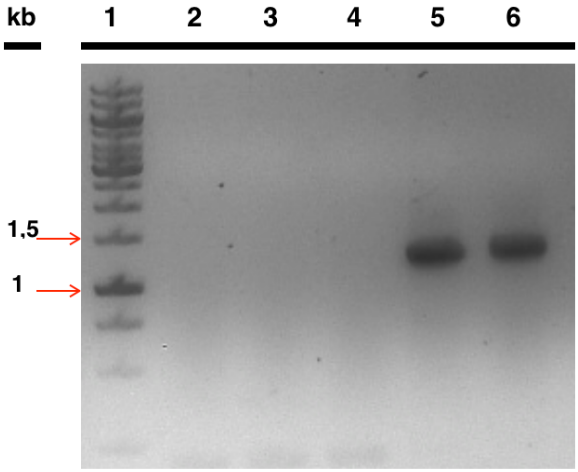

Fig. 9. F1ß-GFP-pcDNA3 *E. coli* colony screening. Lane 1: molecular-weight size marker. Lane 2: clone 31. Lane 3: clone 32. Lane 4: clone 33 . Lane 5: clone 34. Lane 6: clone 35 .

Fig. 9 shows two positive results: clones 34 and 35 (F_1ß-GFPS). Plasmids were extracted and sent for sequencing: F_1ß sequence was conserved.

5.2.3. In vivo expression and immunofluorescence staining

HeLa229 cells were transfected with the extracted plasmids using VIROMER. Two different transfections were performed, one with F_1ß-mCherryS construct (plasmid from clone 2) and the other with F_1ß-GFPS construct (plasmid from clone 34).

To prove the correct localization of F_1ß-mCherryS and F_1ß-GFPS constructs, transfected HeLa229 cells were immunostained with antibodies labeling the outer membrane (anti-Tom20) and the matrix (anti-Prx). Constructs were observed using a confocal microscope and a super resolution microscope. Fig. 10 pictures were taken with Leica TCS SPE confocal microscope and Fig. 11 pictures were taken with SIM Zeiss Elyra. The images displayed were taken of mCherryS-F_1ß transfected HeLa cells. GFPS-F_1ß pictures are not shown.

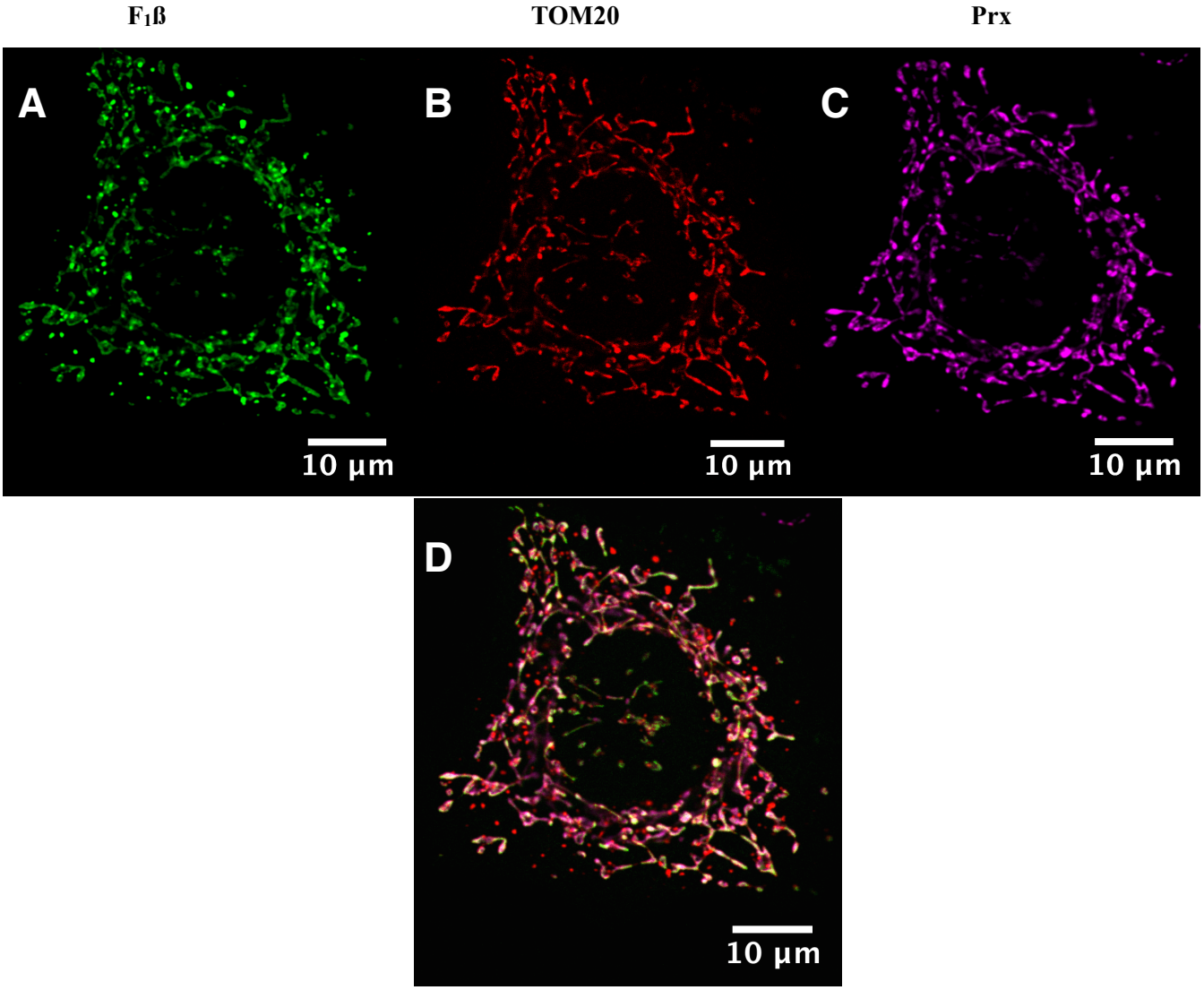

Fig. 10. Confocal picture of fluorescently labelled HeLa229 cell. Leica TCS SPE confocal microscope. Image processed with Fiji [26].
F_1ß-mCherry: green. Tom20: red. Prx: purple. A, B and C pictures show the three different dyes separately. Picture D was obtained superimposing A, B and C.

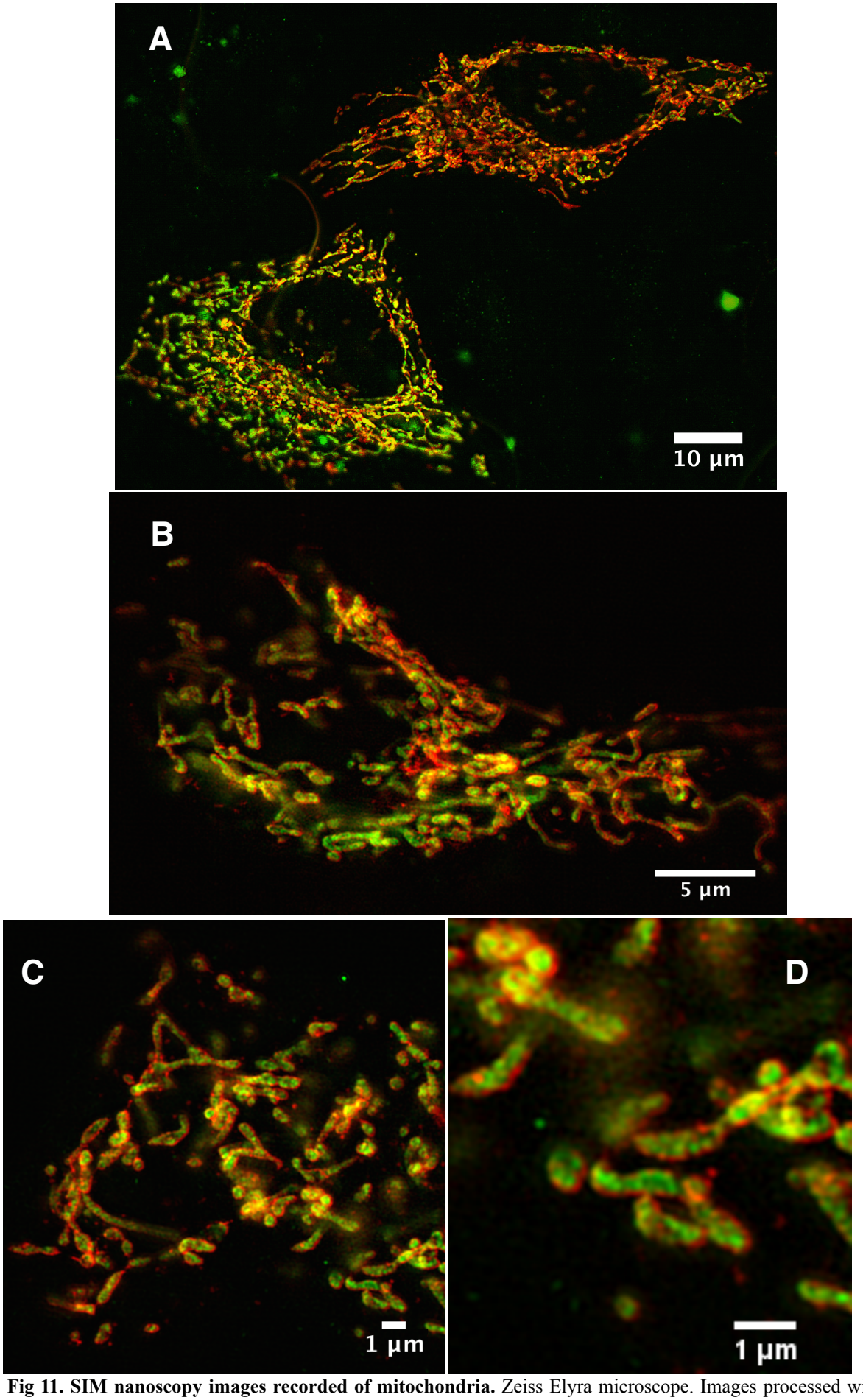

Fig 11. SIM nanoscopy images recorded of mitochondria. Zeiss Elyra microscope. Images processed with Fiji [26].F_1ß-mCherry (green), Tom20 (red). Picture A shows two HeLa transfected cells, mitochondria are distributed through the cytoplasm and the area that presents no fluorescence corresponds to the nucleus. Pictures B, C and D show a close-up of mitochondrium.

6. Discussion

6.1. ZO1 design and amplification

During the design of ZO1 fluorescent fusion protein (FFP), several factors were taken into consideration: the intended use of the FFP, which fluorescent tag to add and where to insert the fluorescent protein **[13]**. As explained before (2.2. and 5.1.), the intended use of ZO1 FFP was to create a construct that could be employed as a tool to study the disruption of tight junctions of the endocervix after *N. gonorrhoeae* infection in 3D models.

The fluorescent tags chosen were GFP and mCherry, with the idea of comparing them after cell transfection and choosing the one that gave the strongest signal. Transfected cells were not obtained, so GFP and mCherry could not be compared. The last point related to the FFP design was where to place the fluorescent protein so it did not affect the localization or functionality of ZO1. As stated before (2.2), ZO1 C-terminal region interacts directly with F-actin and has an important role in the stable localization of ZO1 at tight junctions **[18]**. For this reason, the fluorescent protein was attempted to be fused to the N-terminal region of ZO1.

Standard polymerase chain reaction (PCR) can easily amplify DNA segments smaller than 3 kb, but the amplification of longer templates usually generates variously sized molecules that appear as smears on a gel. To build a fusion protein, the intact DNA is needed, and for this reason the use of comercial systems for long PCR amplification was necessary. From all the systems tested, positive results were only obtained using Phusion Polymerase + DMSO and cDNAa as the template (Fig.5.). cDNAa and cDNAb were extracted from HeLa cells at two different times. Their integrity was checked the same way, amplifying the gene GADPH, a rutine method used at the laboratory. Even though the quality check was positive for both cDNAs, cDNAb ZO1 gene could had been fragmented. This would provide an explanation of why there was no amplification with cDNAb. Another explanation could be that the amounts of mRNA for ZO1 were that low, that there was not enough cDNA in the end to act as a template. *E. coli* were transformed using DISEC-TRISEC but no positive colonies were obtained (plasmid + insert).

Amplification with Aqua-cloning primers was not succesful, maybe due to the primers big length and their melting temperature (Tm). The difference between the Tm of the two was greater than 5 ºC, and the Tm of one of them was 71,2 ºC (Thermo Scientific Tm calculator), which is very close to the optimum extension temperature of phusion polymerase (72ºC). When the annealing temperature is too high, primers are enable to bind to the template.

This is not the first time that creating a ZO1-GFP fusion protein has been attempted. In 2002, a group from the university of Bern designed a ZO1-GFP fusion protein to study the dynamics of tight junctions in living cells. But in this case, ZO1 was amplified from a plasmid containing ZO1 cDNA, instead of using total cDNA. ZO1 was fused to the C-terminal of GFP and it was demonstrated that it didn't affect its localization or function. **[29]**

6.2. Mitochondrial structure and microscopy techniques

Previous studies have already used super resolution microscopy and labeling techniques to visualize submitochondrial structure, some of them focusing on the OMM and others on the IMM. Several of them have used antibodies anti-TOM20 to highlight the OMM or to study the distribution of TOM complexes **[20][21][22]**. On the other hand, studies concerning the IMM have mainly concentrated on OXPHOS (oxidative phosphorylation) proteins, which are very abundant in cristae **[23]**. In this project, both the OMM and the IMM were simultaneously labelled utilizing immunofluorescence and a fusion protein respectively.

Defects in the assembly of OXPHOS proteins in the cristae lead to several human diseases. **[30]**. The ability of visualizing these protein complexes in living cells would contribute to a better understanding of OXPHOS dynamics and its implication in these kind of diseases. As explained in the Background, the best labeling option to study cells "*in vivo*" are fusion proteins. For this reason, F_1ß (forms part of the ATPase complex) was fused to a fluorescent tag instead of immunostaining it. F_1ß has an N-terminal signal presequence that directs it to the mitochondria. Without this signal, it would not be imported to mitochondria and would not be functional, so the fluorescent protein had to be placed at the C-terminal end. Two fluorescent proteins were tested, mCherry and GFP, the fluorescence signal of the constructs was then compared. The best signal was obtained with the mCherryM-F_1ß fusion protein (Fig.9. and Fig.10.). The GFPM-F_1ß images are not shown.

Immunofluorescence staining of the OMM has both served as a comprobation of the high resolution that can be achieved with SIM microscopy and as a colocalization method to prove that the fluorescent tag did not affect F_1ß localization. In the confocal microscope picture (Fig.9), the three colors corresponding to F_1ß (green), TOM20 (red) and Prx (purple) are superimposed, demonstrating that F_1ß is located at mitochondria. SIM pictures (Fig. 10) show the submitochondrial distribution of TOM20 and F_1ß, which, as expected, are located at the OMM and the IMM respectively. Visualization of cristae structure *in vivo* could be used to study their morphology changes under different conditions. For example, during programmed cell death there is a dynamic rearrangement of cristae shape **[31]**. The link has also been established between cristae shape and mitochondrial respiratory efficency. Some studies suggest that cristae shape modulates the organization and function of the OXPHOS system **[32]**.

Comparison of pictures from Fig. 9 and Fig. 10 highlights the difference between confocal microscopy and SIM microscopy. The first one only shows colocalization of the FFP with mitochondria, which for some aplications may be sufficient, whereas the second one permits the visualization of protein distribution in mitochondria. Other studies already mentioned used other types of high resolution microscopy to visualize mitochondria like STORM **[22]** or STED **[20][21][23]**. STED and SIM are both ensemble imaging approaches and they allow the utilization of conventional fluorescent probes, like mCherry or GFP. On the other hand, STORM, is a single-molecule imaging technique, and therefore it requires the use of specific fluorophores **[11]**. Taking these factors into account, SIM can be considered a relatively easy and reliable technique to visualize the submitochondrial structure.

7. Conclusions

The results obtained in this work, allow us to conclude:

1. Phusion polymerase and DMSO permit the amplification of ZO1 cDNA (5,2 kb) from total cDNA.

2. The fluorescent tag does not affect F_1ß fusion protein localization.

3. Confocal microscopy does not allow the visualization of mitochondrial protein distribution, whereas SIM does.

4. The obtained Hela229 transfected cells can be used in future "*in vivo*" or "*in vitro*" essays about mitochondrial protein disrtribution and inner membrane structure and dynamics.

Conclusiones

Los resultados obtenidos en este proyecto, nos permiten extraer las siguientes conclusiones:

1. La polimerasa "Phusion" y el uso de DMSO permiten la amplificación del cDNA de ZO1 (5,2 kb) partiendo de cDNA total.

2. La proteína fluorescente no afecta a la localización de la proteína de fusión de F_1ß.

3. La microscopía confocal no permite la visualización de la distribución submitocondrial de proteínas, mientras que la microscopía SIM sí.

4. Las células HeLa229 transfectadas pueden usarse en ensayos futuros "*in vivo*" o "*in vitro*" sobre la distribución submitocondrial de proteínas y la estructura de la membrana interna y su dinámica.

8. Bibliography

1. Wang LC, Yu Q, Edwards V, Lin B, Qiu J, Turner JR, et al. *Neisseria gonorrhoeae* infects the human endocervix by activating non-muscle myosin II-mediated epithelial exfoliation. PLoS Pathogens. 2017; 13(4): e1006269
2. Devenish RJ, Prescott M, Rodgers AJW. The Structure and Function of Mitochondrial F1F0-ATP Synthases. International Review of Cell and Molecular Biology, 2008; 267: 1-58
3. Schwann T. Mikroskopische Untersuchungen über die Uebereinstimmung in der Struktur und dem Wachsthum der Thiere und Pflanzen, von Dr. Th. Schwann. Berlin: G.E. Reimer, 1839: 191-257.
4. Jakobs S, Wurm CA. Super-resolution microscopy of mitochondria. Current Opinion in Chemical Biology. 2014; 20: 9-15
5. Abbe, E. Beiträge zur Theorie des Mikroskops und der mikroskopischen Wahrnehmung. Archiv für Mikroskopische Anatomie. 1873; 9: 413–418
6. Abramowitz M. Optical Microscopy. Encyclopedia of Imaging Science and Technology, Wiley-Interscience, New York. 2002; 2: 1106-1141.
7. Kopek BG, Shtengel G, Grimm JB, Clayton DA, Hess HF: Correlative photoactivated localization and scanning electron microscopy. PLoS ONE. 2013, 8: e77209.
8. Zhong, G. He J, Zhou R, Lorenzo D, Babcock HP, Bennett V, Zhuang X. Developmental mechanism of the periodic membrane skeleton in axons. eLife 3, 2014: e04581
9. Wurm CA, Neumann D, Lauterbach MA, Harke B, Egner A, Hell SW, Jakobs S. Nanoscale distribution of mitochondrial import receptor Tom20 is adjusted to cellular conditions and exhibits an inner-cellular gradient. Proceedings of the National Academy of Sciences of the United States of America. 2011; 108(33): 13546–13551
10. Yamanaka M, Smith NI, Fujita K. Introduction to super-resolution microscopy. Microscopy. 2014; 63(3): 177-192
11. Huang B, Babcock H, Zhuang X. Breaking the diffraction barrier: Super-resolution imaging of cells. Cell. 2010; 143(7): 1047-1058
12. Giepmans BNG, Adams SR, Ellisman MH, Tsien RY. The fluorescent toolbox for assessing protein location and function. Science. 2006; 312(5771): 217-224
13. Snapp E. Design and Use of Fluorescent Fusion Proteins in Cell Biology. Current Protocols in Cell Biology. 2005; 27(1): 1-13
14. Wang LC, Yu Q, Edwards V, Lin B, Qiu J, Turner JR, Stein DC, Song W. *Neisseria gonorrhoeae* infects the human endocervix by activating non-muscle myosin II-mediated epithelial exfoliation. PLoS Pathogens. 2017; 13(4): e1006269
15. Niessen CM. Tight junctions/adherens junctions: Basic structure and function. Journal of Investigative Dermatology. 2007; 127(11): 2525-2532.
16. Wroblewski LE, Peek RM, Wilson KT. *Helicobacter pylori* and gastric cancer: Factors that modulate disease risk. Clinical Microbiology Reviews. 2010; 23(4): 713-739
17. Fanning AS, Jameson BJ, Jesaitis LA, Anderson JM. The tight junction protein ZO-1 establishes a link between the transmembrane protein occludin and the actin cytoskeleton. Journal of Biological Chemistry. 1998; 273(45): 29745-29753

18. Fanning AS, Ma TY, Anderson JM. Isolation and functional characterization of the actin binding region in the tight junction protein ZO-1. FASEB Journal. 2002; 16(13): 1835-1837

19. Betzig E, Patterson GH, Sougrat R, Lindwasser OW, Olenych S, Bonifacino JS, Davidson MW, Lippincott-Schwartz J, Hess HF. Imaging intracellular fluorescent proteins at nanometer resolution. Science. 2006; 313(5793): 1642-1645

20. Schmidt R, Wurm CA, Jakobs S, Engelhardt J, Egner A, Hell SW. Spherical nanosized focal spot unravels the interior of cells. Nature Methods. 2008; 5(6): 539-544

21. Donnert G, Keller J, Wurm CA, Rizzoli SO, Westphal V, Schönle A, et al. Two-color far-field fluorescence nanoscopy. Biophysical Journal. 2007; 92(8): 67-69

22. Huang B, Jones SA, Brandenburg B, Zhuang X. Whole-cell 3D STORM reveals interactions between cellular structures with nanometer-scale resolution. Nature Methods. 2008; 5(12): 1047-1052

23. Schmidt R, Wurm CA, Punge A, Egner A, Jakobs S, Hell SW. Mitochondrial cristae revealed with focused light. Nano Letters. 2009; 9(6): 2508-2510

24. Wiedemann N, Pfanner N. Mitochondrial Machineries for Protein Import and Assembly. Annual Review Biochemistry. 2017; 86: 685-714

25. Beyer HM, Gonschorek P, Samodelov SL, Meier M, Weber W, Zurbriggen MD. AQUA cloning: A versatile and simple enzyme-free cloning approach. PLoS One. 2015; 10(9): e0137652

26. Schindelin J, Arganda-Carreras I, Frise E, Kaynig V, Longair M, Pietzsch T, Preibisch S, Rueden C, Saalfeld S, Schmid B, Tinevez JY, White DJ, Hartenstein V, Eliceiri K, Tomancak P, Cardona A. Fiji: an open-source platform for biological-image analysis. Nature Methods. 2012; 9(7): 676-682

27. Cheng S, Fockler C, Barnes WM, Higuchi R. Effective amplification of long targets from cloned inserts and human genomic DNA. Proceedings of the National Academy of Sciences of the United States of America. 2006; 91(12): 5695-5699

28. Ohta S, Kagawa Y. Human F1-ATPase: Molecular Cloning of cDNA for the Beta Subunit. Journal of Biochemistry. 1986; 99(1):135–141.

29. Riesen FK, Rothen-Rutishauser B, Wunderli-Allenspach H. A ZO1-GFP fusion protein to study the dynamics of tight junctions in living cells. Histochemistry and Cell Biology. 2002; 117(4): 307-315

30. Smeitink J, Van Den Heuvel L, DiMauro S. The genetics and pathology of oxidative phosphorylation. Nature Reviews Genetics. 2001; 2(5): 342-352

31. Scorrano L, Ashiya M, Buttle K, Weiler S, Oakes SA, Mannella CA, Korsmeyer SJ. A distinct pathway remodels mitochondrial cristae and mobilizes cytochrome c during apoptosis. Developmental Cell. 2002; 2(1): 55-67

32. Cogliati S, Frezza C, Soriano ME, Varanita T, Quintana-Cabrera R, Corrado M, Cipolat S, Costa V, Casarin A, Gomes LC, Perales-Clemente E, Salviati L, Fernandez-Silva P, Enriquez JA, Scorrano L. Mitochondrial cristae shape determines respiratory chain supercomplexes assembly and respiratory efficiency. Cell. 2013; 155(1): 160-171

Supplementary material

Table 1S. Description of the bacterial strain and cell line used.

Bacterial strain//Cell line	**Information**	
***E. coli* strains**		
DH5α	Defined by three mutations: recA1, endA1 (they help plasmid insertion) and lacZM15 (enables blue-white screening).	
Top 10	Ideal for high-efficiency cloning and plasmid propagation. They allow stable replication of high-copy number plasmids.	
Cell lines		**Source**
HeLa 229	Human epithelial cells from a cervical adenocarcinoma	ATCC CCL-2.1
HeLa 2000	Human epithelial cells from a cervical adenocarcinoma	ATCC CCL-227

Table 2S. Cell culture medium

Medium	**Company**
RPMI 1640 GlutaMAXTM-I	GIBCO
FCS	PAA
Ampicillin	Sigma Aldrich

Table 3S. ZO1 primers

Primer	**Sequence**	**Use**
ZO1 forward	AATTCTCCGCCAGAGCT	DISEC-TRISEC
ZO1 reverse	GACTTAAAAGTGGTCAATAAGG	DISEC-TRISEC
ZO1-AQUA forward	GACGAGCTGTACAAGGAATTCTCCGCCAGAGCTGCGGC	AQUA cloning
ZO1-AQUA reverse	CCCTCTAGATGCATGCTCGATTAAAAGTGGTCAATAAG	AQUA cloning

Table 4S. $F_1ß$ primers

Primer	Sequence	Use
$F_1ß$ forward	CTGATGTTGGGGTTTGTG	DISEC-TRISEC
$F_1ß$ reverse	TCGCGATGAATGCTCTTC	DISEC-TRISEC
$F_1ß$-seq-forward	TGGTATATGGTCAAATGAAT	sequencing
$F_1ß$-seq-mCherry-reverse	GAGGAGTCCTGGGTCACGGT	sequencing mCherry plasmid
$F_1ß$-seq-GFP-reverse	TGCGGTTCACCAGGGTGTCG	sequencing GFP plasmid

Table 5S. Equipment used *Falta: termociclador, cubeta electroforesis

Equipment	Company
Electric balance ABS 80-4	Kern
Electrophoresis Power Supply EPS600	Pharmacia Biotech
Hera Cell 240i incubator	Thermo
Herasafe sterile hood	Thermo
Laborvakuumpumpe	Welch
Labtherm ET1311	Liebisch
Magnetic stirrer RMO	Gerhardt
Megafuge 1.0R	Heraeus
Microspin FV-2400	Biosan
NanoDrop 1000 SpeKtrophotometer	Peqlab Biotechnology
Peristaltic pump P-1	Pharmacia Biotech
PowerPack P25T	Biometra
Systec VX-150 autoclave	Systec GmbH
TCS SPE confocal microscope	Leica
Thermocycler	Biorad
Thermo mixer comfort	Eppendorf
Vortex Genie 2™	Bender & Hobeim AG
ZEISS Elyra	ZEISS Microscopy

Acknowledgements

First of all, I would like to thank Dr. Vera Kozjak-Pavlovic from the University of Würzburg for giving me the opportunity of working in her lab and also accepting the task of directing my Bachelor's Thesis, with all that it entails.

I am also grateful to Elke Maier, who showed me how things worked in the laboratory and helped me whenever I asked her.

I would also like to acknowledge Tobias Kunz, who taught me how the confocal and the SIM microscopes worked and helped me taking the pictures that I have used in my thesis.

And finally, last but by no means least, I would like to thank Motaharehsadat Heydarian and Tao Yang, who were always eager to give a helping hand to anyone who needed it.